Stability and Oligosaccharide Binding of the N1 Cellulose-Binding Domain of *Cellulomonas fimi* Endoglucanase CenC†

A. Louise Creagh,[‡,▽] Jürgen Koska,[‡,▽] Philip E. Johnson,[∥] Peter Tomme,[‡,§] Manish D. Joshi,[⊥] Lawrence P. McIntosh,[∥,⊥] Douglas G. Kilburn,[‡,§] and Charles A. Haynes*[,‡,▽]

Protein Engineering Network of Centres of Excellence, The Biotechnology Laboratory and the Departments of Microbiology and Immunology, Chemistry, Biochemistry and Molecular Biology, and Chemical Engineering, University of British Columbia, Vancouver BC, Canada

Received August 11, 1997; Revised Manuscript Received November 25, 1997

ABSTRACT: Differential scanning calorimetry has been used to study the thermal stability and oligosaccharide-binding thermodynamics of the N-terminal cellulose-binding domain of *Cellulomonas fimi* β-1,4-glucanase CenC (CBD_{N1}). CBD_{N1} has a relatively low maximum stability ($\Delta G_{max} = 33$ kJ/mol $= 216$ J/residue at 1 °C and pH 6.1) compared to other small single-domain globular proteins. The unfolding is fully reversible between pH 5.5 and 9 and in accordance with the two-state equilibrium model between pH 5.5 and 11. When the single disulfide bond in CBD_{N1} is reduced, the protein remains unfolded at all conditions, as judged by NMR spectroscopy. This indicates that the intramolecular cross-link makes a major contribution to the stability of CBD_{N1}. The measured heat capacity change of unfolding ($\Delta C_p = 7.5$ kJ mol^{-1} K^{-1}) agrees well with that calculated from the predicted changes in the solvent accessible nonpolar and polar surface areas upon unfolding. Extrapolation of the specific enthalpy and entropy of unfolding to their respective convergence temperature indicates that per residue unfolding energies for CBD_{N1}, an isolated domain, are in accordance with those found by Privalov (*1*) for many single-domain globular proteins. DSC thermograms of the unfolding of CBD_{N1} in the presence of various concentrations of cellopentaose were fit to a thermodynamic model describing the linkage between protein−ligand binding and protein unfolding. A global two-dimensional minimization routine is used to regress the binding enthalpy, binding constant, and unfolding thermodynamics for the CBD_{N1}−cellopentaose system. Extrapolated binding constants are in quantitative agreement with those determined by isothermal titration calorimetry at 35 °C.

Enzymes which degrade carbohydrates, such as cellulases and xylanases, often contain a discrete domain which mediates binding to the polysaccharide and is frequently connected to the catalytic domain by a linker segment rich in proline and threonine (and/or serine). More than 170 cellulose-binding domains (CBDs)[1] have been identified and grouped into 12 different families based on amino acid sequence (*2*). Cellulose-binding domains retain their function when proteolytically separated from the catalytic domain (*3*) or when produced by recombinant gene expression (*4*, *5*). This together with the fact that CBD-fusion proteins retain the activity of the fusion partner (*6*, *7*) makes these binding domains an attractive affinity purification tag that utilizes cellulose as an inexpensive, readily available affinity matrix.

The β-1,4-glucanase CenC from the soil bacteria *Cellulomonas fimi* contains two tandemly repeated N-terminal binding domains, CBD_{N1} and CBD_{N2}, which are members of family IV cellulose binding domains (*2*). Recombinant CBD_{N1} binds soluble cello-oligosaccharides and amorphous (insoluble) cellulose, but not crystalline cellulose (*5*, *8*). This is in contrast to more familiar CBDs from families I to III which are known to bind both amorphous and crystalline cellulose (*9*, *10*) although possibly only to crystalline regions.

The binding of CBD_{N1} to soluble β-1,4-linked glucans and to insoluble amorphous cellulose (*e.g.*, phosphoric acid-swollen cellulose) has been studied by affinity electrophoresis, binding assays and isothermal titration calorimetry (*8*), and by NMR and difference ultraviolet absorbance spectroscopy (*11*). Isothermal titration calorimetry (ITC) results at 35 °C and pH 7 indicate binding constants ranging from 3200 ± 500 M^{-1} for cellotetraose to $24\,000 \pm 4000$ M^{-1} for sugars with 5 or more sequential glucopyranoside units. The binding of CBD_{N1} to cellotetraose, cellopentaose and cellohexaose is 1:1, while three to four CBD_{N1} can bind to

† This work was supported in part by grants from the Natural Sciences and Engineering Research Council of Canada (NSERC) and the Protein Engineering Network of Centres of Excellence (PENCE).

* Author to whom correspondence should be addressed at Biotechnology Laboratory, University of British Columbia, 237-6174 University Blvd., Vancouver BC, Canada V6T 1Z3. E-mail: israels@chml.ubc.ca.

‡ The Biotechnology Laboratory.

§ Department of Microbiology and Immunology.

∥ Department of Chemistry.

⊥ Department of Biochemistry and Molecular Biology.

▽ Department of Chemical Engineering.

[1] Abbreviations: CBD, cellulose-binding domain; CBD_{N1}, N-terminal cellulose-binding domain from the *Cellulomonas fimi* β-1,4-glucanase CenC; C_p, absolute heat capacity; $C_{p,n}$, heat capacity of the native state; C_p^{ex}, excess heat capacity; DSC, differential scanning calorimetry; G5, cellopentaose; HSQC, heteronuclear single quantum correlation; NOE, nuclear Overhauser effect; DTT, dithiothreitol; ΔASA, change in solvent accessible surface area.

S0006-2960(97)01983-1 CCC: $15.00
Published on Web 02/18/1998

each chain of high molecular weight soluble cellulosic polymers. These binding studies, together with NMR-based structural information, suggest that the binding site of CBD_{N1} accommodates *ca.* 5 glucopyranosyl units.

The solution structure of CBD_{N1}, solved by multidimensional multinuclear NMR spectroscopy (*11*, *12*), is a jelly roll β-sandwich with five antiparallel β-strands forming a concave face. Amide chemical shift perturbations and intermolecular NOEs indicate that cello-oligosaccharides bind along this β-sheet cleft. Calorimetry data show that binding of sugars to CBD_{N1} is enthalpically favored with entropy compensation (*8*). NMR data indicate that the binding cleft contains a strip of hydrophobic side chains flanked by polar residues (*12*). Together these data present a binding mechanism whereby CBD_{N1} interacts with β-1,4-linked glucans through both hydrogen bonding to equatorial hydroxyl groups of the pyranose rings and van der Waals stacking of these sugar rings against apolar side chains.

A dependence of ligand binding on the DSC melting thermogram of a protein was first predicted by Schellman (*13*, *14*) using thermodynamic and statistical mechanical methods. He showed that the free energy of interaction of ligands with proteins is a simple function of the coupled unfolding and binding equilibrium constants. The increase in stability of lysozyme to thermal and guanidine hydrochloride denaturation in the presence of tri-*N*-acetylglucosamine (*15*) agreed with Schellman's prediction. Namely, that an increase in stability of an enzyme in the presence of a specific small molecule ligand results because the unfolding equilibrium is shifted to the native state. Similar results have been found using differential scanning calorimetry for several protein−ligand systems (*16*−*21*).

Recently, several methods for determining binding constants using calorimetry have been described (*22*−*27*) and used to characterize protein−ligand interactions (*21*, *28*, *29*). These methods have been successfully applied to both strong and weak protein−ligand interactions. While isothermal titration calorimetry (ITC) will give more precise values for binding constants at temperatures below 50 °C, the DSC method extends the temperature range of validity of binding data and may allow large binding constants (i.e., $> 10^8$ M^{-1}; out of the range of the ITC) to be determined.

In this work, DSC was used to characterize the thermodynamics of the folding-unfolding transition of CBD_{N1} and the effect of oligosaccharide binding on the stability of this protein. A global-minimization algorithm is presented for regressing from DSC data the thermodynamics of linked binding and unfolding reactions based on the excess enthalpy equation of Brandts and Lin (*23*). The algorithm is applied to the thermodynamic characterization of both the thermal stability of CBD_{N1} and the binding of cellopentaose (G5) to CBD_{N1}. There have been several calorimetric studies of the binding of soluble sugar ligands to proteins. These include ITC studies of carbohydrate-binding antibodies (*30*, *31*), glucoamylase (*32*, *33*), lectins (*34*, *35*), and cellulose- and starch-binding domains (*8*, *36*, *37*). Related DSC studies of lysozyme (*15*), L-arabinose-binding protein (*16*), lectin from winged bean (*38*), and maltose-binding protein (*39*) have also been reported. This, however, is the first application of DSC to the characterization of the reversible thermal unfolding (and soluble-sugar binding) of an isolated, well-characterized carbohydrate-binding domain. Beyond its value in our further understanding of carbohydrate-binding proteins, knowledge of stability and binding constants of CBD_{N1} at elevated temperatures will be significant in the application of this domain to affinity purification systems.

MATERIALS AND METHODS

Production and purification of recombinant CBD_{N1} has been described by Tomme et al. (*8*). The molecular weight of the 152-residue protein CBD_{N1} is 15 425 Da.

Cellopentaose (G5) (fine grade, 95+%) was purchased from Seikagaku Corp. (Tokyo). Buffer solutions (50 mM) were prepared from the following salts: pH 4−5, acetic acid (Fisher) and sodium acetate (BDH, 99.5%); pH 6−7, dibasic and monobasic sodium phosphate (Fisher); pH 9−10, glycine (Sigma, 99%) and sodium hydroxide (Fisher); and pH 11, dibasic sodium phosphate and sodium hydroxide (Fisher). All solutions were prepared using distilled water filtered with the Nanopure system.

Differential Scanning Calorimetry

DSC measurements were performed with a Calorimetry Sciences Corp. model 4215 differential scanning calorimeter. Protein samples were exchanged into the appropriate buffer using a 10-mL Amicon ultrafiltration cell with a 1-kDa MWC Omega membrane (Filtron Technology Corp.). The cell was filled 5 times with fresh buffer. The final buffer eluted was used as the reference in the DSC scans. Protein concentrations were determined by UV spectroscopy (280 nm) using the extinction coefficient of 21370 M^{-1} cm^{-1} (*12*). In experiments with G5, the ligand was dissolved in buffer and added to the exchanged protein solution to obtain the desired protein and ligand concentrations. Background excess thermal power scans were obtained with the reference buffer in both sample and reference cells. These were subtracted from the scans for each 0.5-mL sample solution containing 1.5−2.0 mg mL^{-1} CBD_{N1} (at pH 7, the protein concentration was varied between 0.6 and 2.5 mg mL^{-1}) and from 0 to 15 mM G5. All samples were degassed by water-aspirated vacuum for 15 min prior to loading. The scan rate used was 1 °C min^{-1} for all DSC runs reported. Reversibility of unfolding was determined by reheating the sample after cooling in the calorimeter. Scan-rate independence of DSC thermograms was verified for scan rates from 0.25 to 2 °C min^{-1}.

Assignment and subtraction of the native-state heat capacity $C_{p,n}(T)$ from the absolute heat-capacity data $C_p(T)$ to yield C_p^{ex}, the excess heat capacity function, follows the method of Straume and Freire (*26*). In this method, the temperature dependence of $C_{p,n}$ is fit to a linear function as a part of the global minimization routine used to regress unfolding and binding thermodynamics (see Results and Discussion).

NMR Spectroscopy

Uniformly ^{15}N labeled CBD_{N1} was prepared as described previously (*11*). $^1H-^{15}N$ HSQC experiments were recorded using the enhanced-sensitivity pulsed field gradient approach of Kay et al. (*40*). Selective water flip-back pulses were incorporated to minimize the perturbation of the bulk water magnetization (*41*, *42*). The sample conditions were 0.7 mM CBD_{N1} in 50 mM sodium phosphate, 50 mM NaCl, 0.02% NaN_3, pH 6.0, and 10% D_2O/90% H_2O. Spectra were

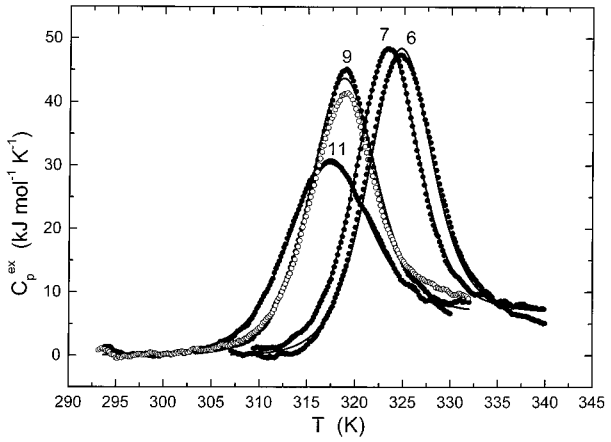

FIGURE 1: DSC thermograms for the unfolding of CBD_{N1} at different pH (values shown above curves) in 50-mM buffer. Filled circles are experimental data for the first scan; open circles are for the second scan at pH 9; lines are nonlinear least-squares fit to a two-state model of unfolding.

acquired with a Varian Unity 500 MHz spectrometer and analyzed using NMRPipe (*43*).

After recording the spectrum of native, oxidized CBD_{N1} at 7 and 35 °C, 100-fold excess (100 mM) of D,L-dithiothreitol (DTT) was added to the sample, followed by a brief period of heating to 90 °C. The spectrum of the reduced protein was then reacquired at 7 and 35 °C. The heating step was utilized to overcome the slow kinetics of disulfide reduction at pH 6. The validity of this approach was confirmed in a separate control experiment carried out with unlabeled CBD_{N1} at pH 8. Under these alkaline conditions, the protein was readily reduced and unfolded at room temperature. After prolonged exposure to air at pH 6 and 8, CBD_{N1} refolded due to loss of the reducing agent and reoxidation of the disulfide bond. The presence of the disulfide was confirmed using native and denaturing polyacrylamide gel electrophoresis. The spectra of reoxidized CBD_{N1} and of CBD_{N1} passed through a cycle of thermal unfolding and refolding in the absence of DTT are identical with that recorded initially for the untreated, native protein. To provide reference spectra for unfolded CBD_{N1}, solid urea and 100 mM DTT were added to an identical sample of the ^{15}N-labeled protein. The final urea concentration was 6.9 M as determined by refractive index measurement.

RESULTS AND DISCUSSION

Thermostability of CBD_{N1}

Figure 1 shows DSC thermograms for *ca.* 0.1-mM solutions of CBD_{N1} in 50-mM buffer at pHs from 6 to 11. The unfolding of CBD_{N1} is fully reversible between pH 5.5 and 9, as shown by the near overlapping thermogram obtained at pH 9 when the sample is reheated. Above pH 9, the unfolding of CBD_{N1} is partially (*ca.* 50%) reversible. Below pH 5.5, however, unfolding is irreversible. Little to no endotherm is obtained upon rescanning the sample, and, at pH 4.6, a white precipitate appears in the cell following the experiment. Aggregation of CBD_{N1} at lower pH is most likely due to the well-established tendency of the solubility of a protein to reach a minimum at or near its isoelectric point (p*I*). Based on primary sequence, the calculated p*I* of CBD_{N1} is 3.5 (*8*).

Table 1: Thermodynamic Parameters for the Native-to-Denatured Transition of CBD_{N1}

pH	T_o (K)	$\Delta H(T_o)$ (kJ mol^{-1})	ΔS(298 K)[a] (kJ mol^{-1} K^{-1})	ΔG(298 K)[a] (kJ mol^{-1})
5.14[b]	324.0(±0.4)	363.6(±18)	0.50(±0.11)	21.1(±1.7)
5.50	323.2	372.1	0.55	21.4
6.10	324.2	410.4	0.64	24.9
7.09	322.5	391.4	0.62	22.5
7.36	321.7	370.4	0.58	20.5
9.06	318.2	361.8	0.65	17.9
10.58[c]	316.7	322.2	0.57	14.7
10.86[c]	316.5	319.4	0.56	14.4
11.06[c]	309.4	295.4	0.68	9.2

[a] Calculated using $\Delta C_p = 7.5$ kJ mol^{-1} K^{-1}. [b] Thermal unfolding was irreversible at pH 5.14 and below. [c] Thermal unfolding was partially reversible at pH 10.58 and above. Average errors in T_o and ΔH calculated as standard deviations from mean value of repeated runs. Errors in ΔS(298 K) and ΔG(298 K) are calculated by propagation of errors analysis.

Data reduction in this work is based on the two-state equilibrium model of Privalov (*44*), which assumes thermodynamic reversibility. Model analysis was therefore restricted to pH 5.5 and above. No concentration or scan-rate dependence of the thermograms was observed over this pH range.

Figure 1 shows the fit of the two-state equilibrium model (*44*) to the unfolding thermograms for CBD_{N1} between pH 6 and 11 (Table 1). Results from the two-state model fit are good, agreeing to within experimental error (±19 kJ/mol) with the calorimetric (peak area) enthalpies of unfolding ΔH_{cal} and with the van't Hoff enthalpy ΔH_{vH} calculated from the shape of the thermogram (*44*):

$$\Delta H_{vH} = \frac{4RT_m^2 \Delta C_p^{max}}{\Delta H_{cal}} \quad (1)$$

where T_m is the temperature at which the heat capacity change relative to baseline is a maximum (ΔC_p^{max}), and R is the gas constant. Between pH 5.5 and 11, the ratio of ΔH_{cal} to ΔH_{vH} is 1.0 ± 0.1, consistent with an equilibrium two-state transition involving a single domain. Below pH 5.5, ΔH_{vH} is greater than ΔH_{cal}, suggesting nonspecific oligomerization of the native-state protein at low pH.

Fukada et al. (*16*) have shown reversible unfolding of L-arabinose binding protein. In addition, Novokhatny and Ingham (*39*) found reversible thermal unfolding of the maltose-binding protein MalE of *Escherichia coli*. Schwarz et al. (*38*) studied the thermal unfolding of the basic lectin from winged bean (WBIA) which binds galactose and its derivatives. Under all conditions, unfolding was only partially reversible. Schwarz et al. (*38*) nevertheless applied the simple reversible mass-action model of Schellman (*13*) to evaluate binding thermodynamics from DSC thermograms in the presence of monomeric derivatives of galactose by assuming denaturation takes place according to the two-step Lumry−Eyring reaction model (*18*) developed for protein denaturation by Sánchez-Ruiz (*45*):

$$N \overset{K_D}{\longleftrightarrow} U \overset{k}{\rightarrow} D \quad (2)$$

where N is the native state, U is the reversibly unfolded state, and D is an irreversibly denatured state. The Sánchez-Ruiz

model is valid for systems where the reversible unfolding reaction occurs rapidly relative to the second, irreversible step over the entire temperature range of the thermal transition. As a result, a true thermodynamic equilibrium between N and U is maintained during the unfolding process and it is possible to extract thermodynamic information from the thermogram (*18*, *46*). Tests for model validity include the presence of partial reversibility upon rescan, and invariance of thermogram shape and position with scan rate. Both criteria hold for the partially reversible thermograms shown in Figure 1 for denaturation of CBD_{N1} between pH 10.6 and pH 11.1.

In contrast to mono- and disaccharide-binding proteins, reversible unfolding of a polysaccharide binding protein has only been shown for the starch-binding domain (SBD) of *Aspergillus niger* glucoamylase. Tanaka et al. (*47*) found the SBD to be the only domain (of five) in the protein to unfold reversibly and according to the two-state equilibrium model, although a complex, somewhat questionable deconvolution algorithm was required to reach this conclusion. No attempt was made by Tanaka et al. to regress unfolding thermodynamics (*e.g.*, Gibbs energies of denaturation) from the deconvoluted thermograms for the SBD.

The heat capacity change of unfolding ΔC_p was calculated from the dependence of $\Delta H(T_o)$ on T_o, where T_o is the melting temperature defined at the midpoint in the unfolding transition, between pH 5.5 and 11. Here, T_o corresponds to T_g in the original model of Schellman (*13*). Within experimental error, ΔC_p is temperature independent throughout the transition regions (35−55 °C) with a regressed value of 7.5(±1.3) kJ mol^{-1} K^{-1}. In theory (*48*), ΔC_p must vary with temperature, but the dependence in this case is too small to measure given the accuracy of the DSC used in these studies. Assuming a constant ΔC_p, the entropy and Gibbs energy changes for the native-to-denatured state transition at 25 °C (Table 1) can be calculated according to the reversible thermodynamic theory of Privalov (*49*)

$$\Delta S(T) = S_D - S_N = \frac{\Delta H(T_o)}{T_o} + \Delta C_p \ln\left(\frac{T}{T_o}\right) \quad (3)$$

$$\Delta G(T) = G_D - G_N = \Delta H(T_o) - T\Delta S(T_o) + \Delta C_p\left[T - T_o - T\ln\left(\frac{T}{T_o}\right)\right] \quad (4)$$

where S_D, for instance, is the entropy of the denatured state.

The Gibbs free energy of stabilization maximum ΔG_{max} corresponds to the unfolding temperature T_s where ΔS is equal to zero so that $T_s = T_o \exp(-\Delta H(T_o)/T_o\Delta C_p)$. Measured unfolding thermograms between pH 5 and 11 indicate that the thermal stability of CBD_{N1} is a maximum at *ca.* pH 6.1. Figure 2 shows calculated reversible unfolding energies and entropies against temperature at pH 6.1 (assuming a constant ΔC_p = 7.5 kJ mol^{-1} K^{-1}). At 1 °C, the native-state protein reaches its maximum stability of 33 kJ mol^{-1}, which is equivalent to a per residue Gibbs energy change of 216 J mol^{-1}. Becktel and Schellman (*48*) have argued that the maximum stability of globular proteins should normally lie between 200 and 500 J (mol residue)$^{-1}$. Thus, CBD_{N1} has a relatively low maximum stability compared to other

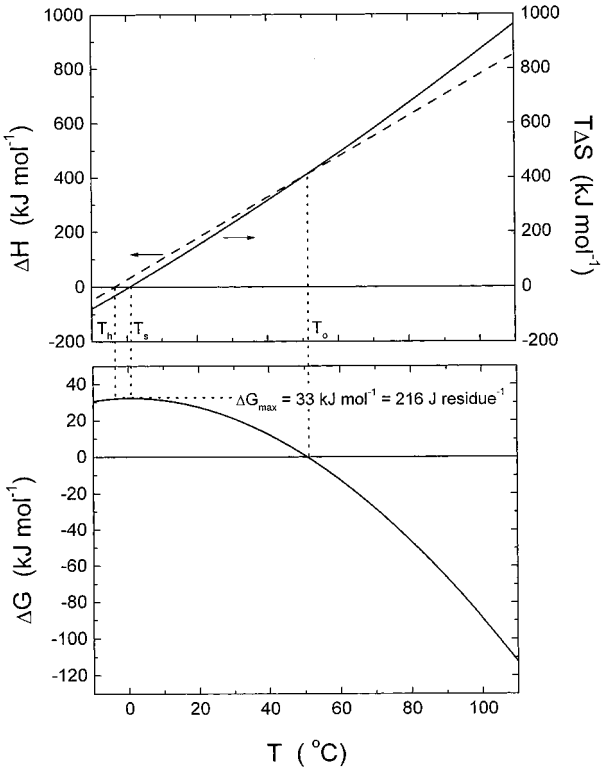

FIGURE 2: Enthalpy (dashed line), entropy (solid line), and Gibbs energy changes for the native-to-denatured state transition of CBD_{N1} at pH 6.1.

(small) globular proteins. Although data are limited, it appears that a low maximum stability may be a common characteristic of sugar-binding proteins. Maltose-binding protein, for instance, has a maximum stability of only 95 J (mol residue)$^{-1}$ which occurs at a relatively high temperature of 28 °C (*39*), and arabinose-binding protein has a maximum stability of 160 J (mol residue)$^{-1}$ at 9 °C (*16*).

Becktel and Schellman (*48*) and, most notably, Pace and Laurents (*50*) have also argued that the value of T_s, which typically falls between −10 and 35 °C, is indicative of the polarity of a protein. Although the complex dependence of ΔG_{max} (and T_s) on numerous system variables renders such an analysis only qualitative at best, relatively hydrophilic proteins such as RNAse T1 usually exhibit low T_s values (<5 °C) while hydrophobic proteins have T_s values near 35 °C (*50*). The low temperature of maximum stability observed for CBD_{N1} (1 °C) suggests that the interior of the protein is relatively hydrophilic (see next section).

Due to the opposite temperature dependencies of the enthalpies of transfer of polar and nonpolar groups from the protein interior into water upon unfolding, the specific enthalpies of unfolding of single-domain globular proteins tend to approach a common value of *ca.* 55 J g^{-1} when extrapolated to the enthalpy convergence temperature T_H* (*44*). A similar argument holds for the unfolding entropy ΔS so that a universal value of the specific entropy of unfolding of *ca.* 0.135 J g^{-1} K^{-1} is often found at an entropy convergence temperature T_S* which is observed (but not theoretically proven) to be essentially equal to T_H* (*1*, *51*, *52*). If a temperature independent value of ΔC_p is used, both T_H* and T_S* are about 110 °C. (Privalov and Makhatadze (*53*) have argued that this value should increase to about 130 °C when the temperature dependence of ΔC_p is

considered.) The extrapolated specific enthalpy and entropy of unfolding for CBD_{N1} at 110 °C (using a constant ΔC_p of 7.5 kJ mol^{-1} K^{-1}) are 55.2 J g^{-1} and 0.163 J g^{-1} K^{-1}, respectively, indicating that CBD_{N1} unfolds like a single-domain globular protein and suggesting that it may serve as an excellent model system for studying structure−stability−function relationships in carbohydrate-binding reactions.

Predicted Changes in Accessible Polar and Apolar Surface Area upon Unfolding

Several similar methods have been proposed for calculating thermodynamic properties of protein unfolding based on model compound studies utilizing the change in solvent accessible nonpolar ΔASA_{NP} and polar ΔASA_P surface area (*54*−*58*). We compared our results for the unfolding of CBD_{N1} to those calculated by the liquid hydrocarbon/amide model of Spolar et al. (*57*) and by the solid cyclic dipeptide model of Murphy and Freire (*56*). The predicted changes in nonpolar and polar surface areas for the unfolding of CBD_{N1} are 8076 and 3383 Å^2, respectively. These values were calculated with the program VADAR (*59*) using the Lee and Richards (*60*) algorithm. The native state is taken as the mean minimized NMR structure of CBD_{N1} (*12*). The unfolded state is modeled as an extended (β-form) structure with backbone ϕ and ψ angles of −140° and +140°, respectively. Combining these results with the hydrocarbon/amide model of Spolar et al. (*57*) gives a theoretical ΔC_p of 8.3 kJ mol^{-1} K^{-1}, in reasonably good agreement with our calorimetric values. Similar results were obtained with the model of Murphy and Freire (*56*).

In the previous section, we argued that the low value of T_s (1 °C) for CBD_{N1} suggests that it is a relatively hydrophilic protein. Expressing the heat-capacity correlation of Spolar et al. (*57*) on a per residue basis (where N_r is the number of residues), denoted by *,

$$\Delta C_p^* \text{ (J (mol residue)}^{-1}\text{ K}^{-1}) = \frac{1}{N_r}(1.34\Delta ASA_{NP} - 0.586\Delta ASA_p) \quad (5)$$

$$= 1.34\Delta ASA_{NP}^* - 0.586\Delta ASA_P^*$$

removes molecular weight effects and thereby should provide a quantitative scale of interior protein hydrophilicity. As shown in eq 5, ΔC_p^* decreases with increasing interior protein hydrophilicity. Hydrophilic proteins, irrespective of their molecular weight, should therefore be characterized by a quantitatively similar, relatively low value of ΔC_p^*; all hydrophobic proteins should yield a comparatively high value of ΔC_p^*. Figure 3 plots measured per residue heat-capacity data taken from this work and Spolar et al. (*57*) as a function of ΔASA_{NP}^* (Å^2 (mol residue)$^{-1}$). ΔC_p^* varies from *ca.* 42 J (mol residue)$^{-1}$ K^{-1} for hydrophilic proteins such as RNase A (*61*) to 73.5 J (mol residue)$^{-1}$ K^{-1} for very hydrophobic proteins such as maltose-binding protein (*39*). Reexpressing the heat-capacity correlation of Spolar et al. (*57*) according to eq 5 therefore increases the information content of their correlation to include a gauge of protein hydrophobicity. A striking example of this is given by the measured ΔC_p (not included in the original analysis of Spolar et al.) for the two strongly hydrophobic proteins, *Staphylococcus* nuclease (ΔC_p = 10.9 kJ mol^{-1} K^{-1}; *62*) and maltose-binding protein (ΔC_p = 27.2 kJ mol^{-1} K^{-1}; *39*). Although there is a more than a 2-fold difference in ΔC_p values, ΔC_p^* is nearly identical for the two proteins: 71.1 and 73.5 J (mol residue)$^{-1}$ K^{-1}, respectively.

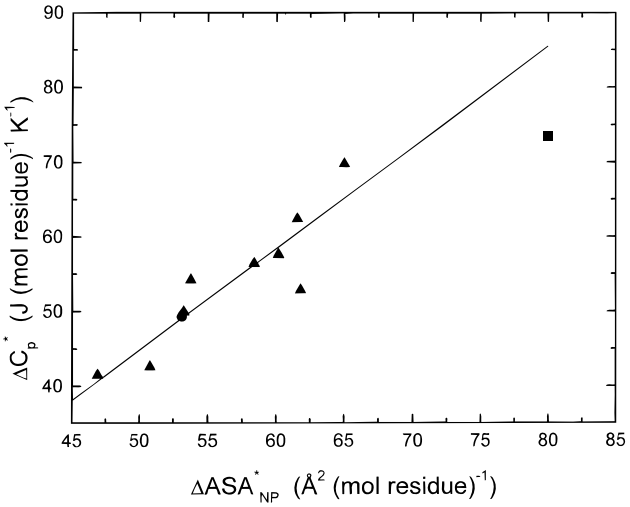

FIGURE 3: Per residue heat capacity change upon unfolding as a function of the per residue change in apolar solvent-accessible surface area: ▲, ■, and ● are data of Spolar et al. (*57*) for various globular proteins, data of Novokhatny and Ingham (*39*) for maltose binding protein, and our results for CBD_{N1}, respectively. Line represents least-squares linear fit of the data of Spolar et al. (*57*).

The measured ΔC_p for unfolding of CBD_{N1} yields a per residue heat capacity change ΔC_p^* of 49.3 J (mol residue)$^{-1}$ K^{-1}. As indicated in Figure 3, CBD_{N1} is among the more hydrophilic single-domain proteins studied to date. Inspection of the sequence of CBD_{N1} reveals a slight excess of hydrophilic amino acids (defined here to include D, E, H, K, N, P, Q, R, S, T) over hydrophobic (A, C, F, G, I, L, M, V, W, Y), with an unusually high number of threonines. Interestingly, CBD_{N1} contains 21 acidic residues (D, E) yet only three basic residues (R).

Contribution of the Disulfide Bond to Stability

CBD_{N1} has one disulfide bond between Cys33 and Cys140. This intramolecular cross-link bridges two β-strands on the sheet opposite the binding face of the domain (*12*). The position of the exposed disulfide bond suggests that it serves to stabilize the folded state rather than to direct the precise structure of the binding site. Figure 4 shows $^1H-^{15}N$ HSQC NMR spectra for CBD_{N1} at 35 °C in both its oxidized and reduced forms. Each peak in the spectra corresponds to a $^1H-^{15}N$ pair in the backbone and side chains of the protein, and as such is an exquisitely sensitive measure of conformation. The spectra for reduced and oxidized CBD_{N1} in 7-M urea at 35 °C are also shown to provide fingerprints of the fully denatured state. Reduction of the disulfide bond with 100-mM DTT (*ca.* 100-fold excess with respect to CBD_{N1}) results in complete denaturation of CBD_{N1} as reflected in the close similarity of the collapsed spectrum with those measured for the protein in 7-M urea. Although subtle differences can be seen between the three spectra of the unfolded protein, we have no evidence for significant residual structure in the reduced protein. Reoxidation of the reduced

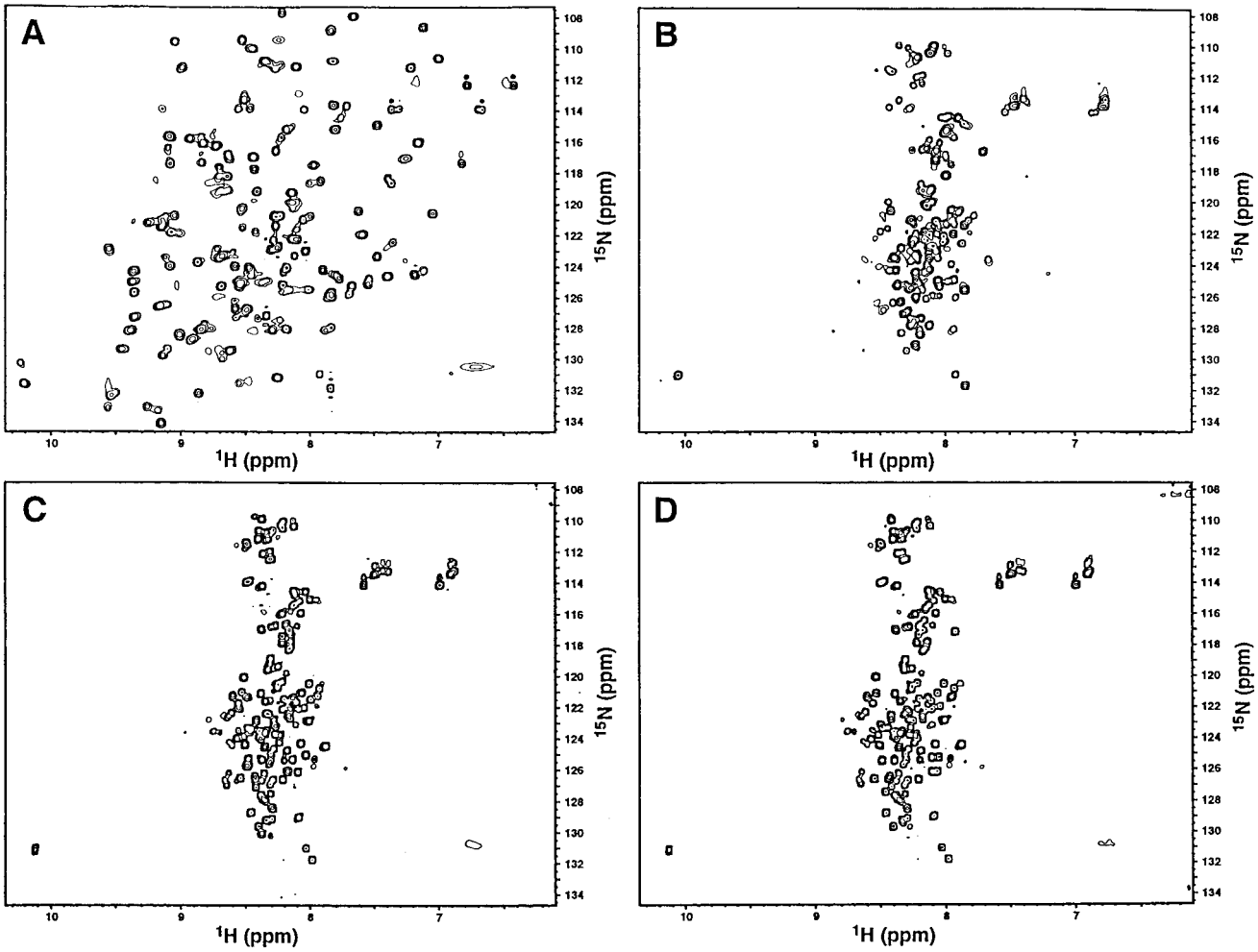

FIGURE 4: $^{1}H-^{15}N$ HSQC NMR spectra at 35 °C and pH 6 of (A) native, oxidized CBD_{N1}, and of CBD_{N1} denatured by (B) reduction, (C) addition of 7-M urea (oxidized), and (D) reduction in the presence of 7-M urea.

sample leads to quantitative refolding of the domain to its native state. It is noteworthy that the unfolded, reduced CBD_{N1} remains fully soluble at NMR concentrations in the absence of added denaturant. This is consistent with the hydrophilic nature of CBD_{N1} and its ability to undergo reversible thermal unfolding.

Lowering the solution temperature of the reduced protein sample to 7 °C, which is near T_s (1 °C), does not result in measurable refolding. This indicates that the disulfide bond makes a substantial contribution to the stability of CBD_{N1}. At 7 °C, ΔG of unfolding of the native (oxidized) structure is 33 kJ mol^{-1} (see Figure 2). Thus, the cumulative effects of reducing the single Cys33 to Cys140 disulfide bond lead to a reduction in folded-state stability $\Delta(\Delta G)$ of at least that amount.

It is generally assumed that disulfide bonds stabilize folded proteins, at least in part, by restricting the conformational freedom of the unfolded state (*63*, *64*). On the basis of a random-coil polymer result of Flory (*65*), Pace et al. (*66*) have suggested that a good estimate of this conformational entropy loss ΔS_{conf} (J mol^{-1} K^{-1}) accompanying formation of a disulfide bond can be obtained from

$$\Delta S_{conf} = -4.184(2.1 - {}^{3}/_{2}R \ln n) \qquad (6)$$

where n is the number of residues between the cross-linked side chains. Equation 6, which strictly applies only to a single polypeptide chain in a random-coil configuration, predicts that the reduction in conformational entropy upon oxidation will increase, thereby enhancing the stability of the folded state, with greater separation of the cysteines in the primary sequence. This effect has been confirmed qualitatively by Zhang et al. (*42*) using cyclic permutation of the N- and C-termini of disulfide-bridged variants of T4 lysozyme. Nevertheless, proteins containing a disulfide bridge which connects cysteines separated by more than 100 intervening amino acids are relatively rare. Srinivasan et al. (*67*) found that the number of residues between cysteines varied from 4 to 129 with two distinct peaks in the distribution of loop sizes: a broad peak between 10 and 30 residues (*68*), and a sharp peak between 60 and 70 residues. CBD_{N1} contains a single disulfide bridge which forms a 108-amino acid loop. This effectively joins the chain near the carboxy and amino termini, making it a good model for assessing the limit to which forming a single disulfide bond can decrease the conformational entropy of the unfolded state. Enthalpic contributions to hydrophobic dehydration generally approach zero at 300 K (*49*). Application of eq 6 yields a value for $-T\Delta S_{conf}$ at 300 K of *ca.* 20.2 kJ mol^{-1}, which is of the same order as the minimum $\Delta(\Delta G)$ change ($>$24 kJ mol^{-1}) resulting from formation of the disulfide bond at this temperature.

On the basis of solvent transfer experiments for model compounds, Doig and Williams (*69*) argue that cross-links *destabilize the folded state entropically* despite the large reduction in conformational freedom (ΔS_{conf}) of the denatured (oxidized) polypeptide chain. This somewhat surprising assertion, which conflicts with the conclusions of Pace et al. (*66*), suggests that the observed overall stabilization of the folded state is instead an enthalpic consequence of significantly less water being required to solvate the denatured protein in its oxidized form. For a small loop, the argument of Doig and Williams seems reasonable since the peptide region bounded by the cysteines in the denatured reduced state is likely to contain a smaller number of intraprotein interactions. Experimental validation of the model for small loops has come from DSC studies of modifying the Cys77−Cys95 loop of human lysozyme (*70*) and the Cys14−Cys38 loop of bovine pancreatic trypsin inhibitor (*71*). In both cases, ΔH(298 K) was higher for the cross-linked protein, which must occur if the disulfide bridge entropically destabilizes the folded state.

The argument of Doig and Williams, however, is less convincing when a large loop is considered, as in the case of CBD_{N1}. Dill and Shortle (*72*), for instance, contend that denatured chain conformations can contain regions of significant (solvent-excluded) structure, a result which is finding increasing support from solution NMR data (*73*). It is therefore difficult to argue that formation of a single disulfide bridge between distant cysteines will neccessarily lead to a lower net hydration of apolar surface area in the denatured state. For hen egg-white lysozyme, Cooper et al. (*74*) have shown that reduction of the Cys6−Cys127 disulfide bridge reduces ΔG(298 K) by *ca.* 28 kJ mol^{-1} without an observed change in ΔH. Our results are consistent with these and the arguments of Pace et al. (*66*). They suggest that for large loops, the loss in stability resulting from reduction of the disulfide bridge can be attributed to an increase in the entropy difference between the denatured and folded structures.

Thermal Unfolding of CBD_{N1} in the Presence of Cellopentaose

Figure 5 shows DSC thermograms for the unfolding of CBD_{N1} in the presence of G5. As predicted by Schellman (*13*, *14*), binding of G5 to native-state CBD_{N1} increases the thermal stability of the protein as measured by T_m. A simple mass-action based model derived by Fukada et al. (*16*) has been used in several studies (*17*, *38*, *47*) to estimate the van't Hoff binding enthalpy and its temperature dependence from this shift in the observed transition region with increasing ligand concentration. The theory does not, however, allow for straightforward regression of the binding constant (i.e., ΔG_b, where subscript b denotes binding).

A more exact route to determining binding thermodynamics from DSC data is through the excess heat capacity $C_p^{ex}(T)$, which is the direct thermodynamic observable in the DSC thermogram. Assuming all transitions are two-state and the ligand binds only to the native state, Brandts and Lin (*23*) derived the following expression for the excess enthalpy $H^{ex}(T)$ accompanying reversible protein unfolding in the presence of ligand:

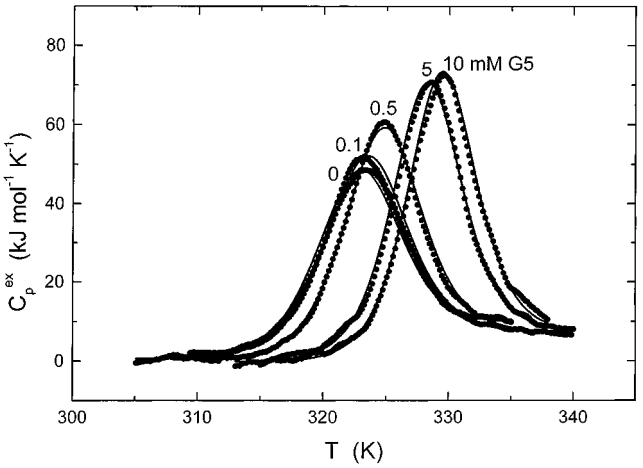

FIGURE 5: DSC thermograms of the unfolding of CBD_{N1} in the presence of various concentrations of G5 (concentrations (mM) shown above curves), 50-mM phosphate buffer, pH 7.09. Filled circles are experimental data; lines are nonlinear least-squares global fit of eq 10 describing coupled ligand binding and protein unfolding (see eq 7). The thermal unfolding temperature T_o in the absence of ligand is 49 °C, where $K_b = 3500$ M^{-1} and $\Delta H_b = -53$ kJ mol^{-1}.

$$H^{ex}(T) = \frac{[P']}{P_t}[\Delta H(T_o) + \Delta C_p(T - T_o)] + \frac{[PL]}{P_t}[\Delta H_b(T_o) + \Delta C_{pb}(T - T_o)] \quad (7)$$

where [P′] is the unfolded protein concentration, P_t is the total protein concentration, and [PL] is the concentration of bound folded protein. In eq 7, [P′]/P_t represents the fraction of denatured protein, where [P′] is defined by the equilibrium unfolding reaction

$$P \leftrightarrows P' \qquad K = \frac{[P']}{[P]} \quad (8)$$

which is characterized by a standard-state denaturation enthalpy change $\Delta H(T_o)$ and heat-capacity change $\Delta C_p(T_o)$. The fraction of bound protein, [PL]/P_t, diminishes to zero as the denaturation reaction proceeds according to eq 8 and the equilibrium binding reaction

$$P + L \leftrightarrows PL \qquad K_b = \frac{[PL]}{[P][L]} \quad (9)$$

characterized by a binding enthalpy $\Delta H_b(T_o)$ and heat capacity $\Delta C_{pb}(T_o)$.

Differentiation of $H^{ex}(T)$ with respect to temperature gives C_p^{ex}

$$C_p^{ex} = \left(\frac{\partial H^{ex}(T)}{\partial T}\right)_{p,x} \quad (10)$$

which, when combined with the equations for conservation of mass of protein and ligand, can be directly regressed to the set of DSC thermograms for CBD_{N1} in the presence of G5 shown in Figure 5 provided an appropriate fitting algorithm is established.

The excess heat-capacity function was fit to the experimental data by minimizing the least squares residual χ^2

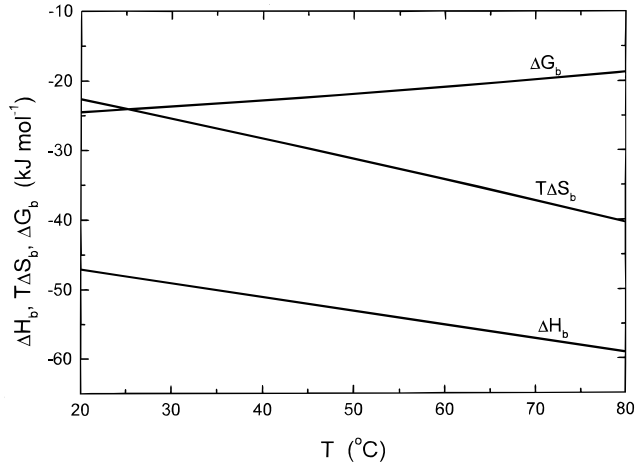

FIGURE 6: Calculated enthalpy, entropy and Gibbs energy change for the binding of G5 to CBD_{N1} at pH 7 as determined from the DSC data.

$$\chi^2 = \sum_{i=1}^{n_p} w_i((C_p^{ex})^{obs} - (C_p^{ex})^{calc})^2 \qquad (11)$$

where $(C_p^{ex})^{obs}$ and $(C_p^{ex})^{calc}$ are the measured and calculated values, respectively, n_p is the number of experimental data points, and w_i is the weighting factor associated with each point. In the present analysis, all weighting factors were set equal to unity to preserve thermodynamic consistency. The nonlinear set of equations which result from eq 11 is solved by a Gauss−Newton method incorporating the Levenberg−Marquardt modification (*75*) to ensure rapid convergence and a second-order accurate numerical differentiation scheme to calculate the gradient matrix.

Results of the nonlinear least-squares global fitting of eq 10 to the set of DSC thermograms measured in the presence of G5 are shown in Figure 5. $(C_p^{ex})^{calc}$ contains seven parameters which must be known or regressed. Four of these parameters [$\Delta H(T_o)$, $K(T_o)$, $\Delta C_p(T_o)$, and T_o] were taken from DSC results for CBD_{N1} in the absence of ligand (see Table 1). The remaining three parameters [$\Delta H_b(T_o)$, $K_b(T_o)$, and $C_{pb}(T_o)$] were regressed. The results of the global fitting gave values for $K_b(T_o)$ and $\Delta H_b(T_o)$ of 3500 M^{-1} and −53 kJ mol^{-1}, respectively. χ^2 was insensitive to the value of $\Delta C_{pb}(T_o)$, making it impossible to directly regress this parameter. However, a value for ΔC_{pb} at 35 °C of −0.21 kJ mol^{-1} K^{-1} has been previously measured by isothermal titration calorimetry (*8*). This value of ΔC_{pb} was therefore assumed to be temperature independent and used in our analysis.

Figure 6 shows the temperature dependence of ΔG_b, ΔH_b, and $T\Delta S_b$ as calculated from our DSC data. At 35 °C, the values extrapolated from our global-fitting analysis (ΔG_b(35 °C) = 23.6 kJ mol^{-1} and ΔH_b = −50 kJ mol^{-1}) agree well with those determined using isothermal titration calorimetry (ΔG_b(35 °C) = 25.5 ± 2.7 kJ mol^{-1} and ΔH_b = −53.0 ±1.3 kJ mol^{-1}) by Tomme et al. (*8*). The increase in the enthalpic driving force for binding with increasing temperature, combined with the concomitant strong decrease (i.e., greater loss) in entropy, suggests that the degree of structure of the hydration layer on the protein- and ligand-binding surfaces prior to binding makes a significant contribution to the overall binding energetics. At elevated temperatures, we would expect the degree of ordering of the hydration layer to be reduced, so that the dominant entropic effect becomes the loss in conformational freedom of the sugar chain upon binding.

ACKNOWLEDGMENT

The authors thank R. Anthony Warren, Neil Gilkes, and Emmanuel Brun for helpful discussions. Koman Joe is also thanked for assisting in control studies of the role of the disulfide in CBD_{N1}.

REFERENCES

1. Makhatadze, G. I., and Privalov, P. L. (1993) *J. Mol. Biol. 232*, 639−659.
2. Tomme, P., Warren, R. A. J., Miller, R. C., Jr., Kilburn, D. G., and Gilkes, N. R. (1995) in *Enzymatic Degradation of Insoluble Polysaccharides* (Saddler, J. N., and Penner, M., Eds.) pp 142−163, American Chemical Society, Washington, DC.
3. Gilkes, N. R., Warren, R. A. J., Miller, R. C., Jr., and Kilburn, D. G. (1988) *J. Biol. Chem. 263*, 10401−10407.
4. Greenwood, J. M., Gilkes, N. R., Kilburn, D. G., Miller, R. C., Jr., and Warren, R. A. J. (1989) *FEBS Lett. 244*, 127−137.
5. Coutinho, J. B., Gilkes, N. R., Warren, R. A. J., Kilburn, D. G., and Miller, R. C., Jr. (1992) *Mol. Microbiol. 6(9)*, 1243−1252.
6. Ong, E., Gilkes, N. R., Warren, R. A. J., Miller, R. C., Jr., and Kilburn, D. G. (1989) *Bio/Technology 7*, 604−607.
7. Greenwood, J. M., Ong, E., Gilkes, N. R., Warren, R. A. J., Miller, R. C., Jr., and Kilburn, D. G. (1992) *Protein Sci. 5*, 361−365.
8. Tomme, P., Creagh, A. L., Kilburn, D. G., and Haynes, C. A. (1996) *Biochemistry 35*, 13885−13894.
9. Gilkes, N. R., Jervis, E., Henrissat, G., Tekant, B., Miller, R. C., Jr., Warren, R. A. J., and Kilburn, D. G. (1992) *J. Biol. Chem. 267*, 6743−6749.
10. Ong, E., Gilkes, N. R., Miller, R. C., Jr., Warren, R. A. J., and Kilburn, D. G. (1993) *Biotechnol. Bioeng. 42*, 401−409.
11. Johnson, P. E., Tomme, P., Joshi, M. D., and McIntosh, L. P. (1996) *Biochemistry 35*, 13895−13906.
12. Johnson, P. E., Joshi, M. D., Tomme, P., Kilburn, D. G., and McIntosh, L. P. (1996) *Biochemistry 35*, 14381−14394.
13. Schellman, J. A. (1975) *Biopolymers 14*, 999−1018.
14. Schellman, J. A. (1976) *Biopolymers 15*, 999−1000.
15. Pace, C. N., and McGrath, T. (1980) *J. Biol. Chem. 255*, 3862−3865.
16. Fukada, H., Sturtevant, J. M., and Quiocho, F. A. (1983) *J. Biol. Chem. 258*, 13193−13198.
17. Edge, V., Allewell, N. M., and Sturtevant, J. M. (1985) *Biochemistry 24*, 5899−5906.
18. Manly, S. P., Matthews, K. S., and Sturtevant, J. M. (1985) *Biochemistry 24*, 3842−3846.
19. Ghosaini, L. R., Brown, A. M., and Sturtevant, J. M. (1988) *Biochemistry 27*, 5257−5261.
20. Schwarz, F. P. (1988) *Biochemistry 27*, 8429−8436.
21. Martínez, J. C., El Harrous, M., Filimonov, V. V., Mateo, P. L., and Fersht, A. R. (1994) *Biochemistry 33*, 3919−3926.
22. Robert, C. H., Gill, S. J., and Wyman, J. (1988) *Biochemistry 27*, 6829−6835.
23. Brandts, J. F., and Lin, L.-N. (1990) *Biochemistry 29*, 6927−6940.
24. Shrake, A., and Ross, P. D. (1990) *J. Biol. Chem. 265*, 5055−5059.
25. Shrake, A., and Ross, P. D. (1992) *Biopolymers 32*, 925−940.
26. Straume, M., and Freire, E. (1992) *Anal. Biochem. 203*, 259−268.
27. Barone, G., Del Vecchio, P., Fessas, D., Giancola, C., Graziano, G., and Ricco, A. (1994) *J. Thermal Anal. 41*, 1263−1276.

28. Hu, C.-Q., and Sturtevant, J. M. (1992) *J. Phys. Chem. 96*, 4052−4056.
29. Barone, G., Catanzano, F., Del Vecchio, P., Giancola, C., and Graziano, G. (1995) *Pure Appl. Chem. 67(11)*, 1867−1872.
30. Sigurskjold, B. W., and Bundle, D. R. (1992) *J. Biol. Chem. 267*, 8371−8376.
31. Brummell, D. A., Sharma, V. P., Anand, N. N., Bilous, D., Dubuc, G., Michniewicz, J., MacKenzie, C. R., Sadowska, J., Sigurskjold, B. W., Sinnott, B., Young, N. M., Bundle, D. R., and Narang, S. A. (1993) *Biochemistry*, *32*, 1180−1187.
32. Sigurskjold, B. W., Berland, C. R., and Svensson, B. (1994) *Biochemistry 33*, 10191−10199.
33. Berland, C. R., Sigurskjold, B. W., Stoffer, B., Frandsen, T. P., and Svensson, B. (1995) *Biochemistry 34*, 10153−10161.
34. Bains, G., Lee, R. T., Lee, Y. C., and Freire, E. (1992) *Biochemistry 31*, 12624−12628.
35. Chervenak, M. C., and Toone, E. J. (1995) *Biochemistry*, *34*, 5685−5695.
36. Sigurskjold, B. W., Svensson, B., Williamson, G., and Driguez, H. (1994) *Eur. J. Biochem. 225*, 133−141.
37. Creagh, A. L., Ong, E., Jervis, E., Kilburn, D. G., and Haynes, C. A. (1996) *Proc. Natl. Acad. Sci. U.S.A. 93*, 12229−12234.
38. Schwarz, F. P., Puri, K., and Surolia, A. (1991) *J. Biol. Chem. 266*, 24344−24350.
39. Novokhatny, V., and Ingham, K. (1997) *Protein Sci. 6*, 141−146.
40. Kay, L., Keifer, P., and Saarinen, T. (1992) *J. Am. Chem. Soc. 114*, 10663−10665.
41. Grzesiek, S., and Bax, A. (1993) *J. Am. Chem. Soc. 115*, 12593−12594.
42. Zhang, O., Kay, L. E., Olivier, J. P., and Foreman-Kay, J. D. (1994) *J. Biomol. NMR 4*, 845−858.
43. Delaglio, F., Grzesiek, S., Vuister, G. W., Zhu, G., Pfeifer, J., and Bax, A. (1995) *J. Biomol. NMR 6*, 277−294.
44. Privalov, P. L. (1979) *Adv. Protein Chem. 33*, 167−239.
45. Sánchez-Ruiz, J. M. (1992) *Biophys. J. 61*, 921−935.
46. Sánchez-Ruiz, J. M., López-Lacomba, J. L., Cortijo, M., and Mateo, P. L. (1988) *Biochemistry 27*, 1648−1652.
47. Tanaka, A., Fukada, H., and Takahashi, K. (1995) *J. Biochem. 117*, 1024−1028.
48. Becktel, W. J., and Schellman, J. A. (1987) *Biopolymers 26*, 1859−1877.
49. Privalov, P. L. (1989) *Annu. Rev. Biophys. Chem. 18*, 47−69.
50. Pace, C. N., and Laurents, D. V. (1989) *Biochemistry 28*, 2520−2525.
51. Baldwin, R. L., and Muller, N. (1992) *Proc. Natl. Acad. Sci. U.S.A. 89*, 7110−7113.
52. Doig, A. J., and Williams, D. H. (1992) *Biochemistry 31*, 9371−9375.
53. Privalov, P. L., and Makhatadze, G. I. (1993) *J. Mol. Biol. 232*, 660−679.
54. Baldwin, R. L. (1986) *Proc. Natl. Acad. Sci. U.S.A. 83*, 8069−8072.
55. Privalov, P. L., and Makhatadze, G. I. (1990) *J. Mol. Biol. 213*, 385−391.
56. Murphy, K. P., and Freire, E. (1992) *Adv. Protein Chem. 43*, 313−361.
57. Spolar, R. S., Livingstone, J. R., and Record, M. T. (1992) *Biochemistry 31*, 3947−3955.
58. Khechinashvili, N. N., Janin, J., and Rodier, F. (1995) *Protein Sci. 4*, 1315−1324.
59. Wishart, D. S., Willard, L., Richards, F. M., and Sykes, B. D. (1995) *VADAR: A comprehensive program for protein structure evaluation. Version 1.2*, University of Alberta, Edmonton, Canada.
60. Lee, B., and Richards, F. M. (1971) *J. Mol. Biol. 55*, 379−400.
61. Privalov, P. L., Tiktopulo, E. I., and Khechinashvili, N. N. (1973) *Int. J. Peptide Protein Res. 5*, 229−237.
62. Calderon, R. O., Stolowich, N. J., Gerlt, J. A., and Sturtevant, J. M. (1985) *Biochemistry 24*, 6044−6049.
63. Creighton, T. E., Zapun, A., and Darby, N. J. (1995) *Trends Biotechnol. 13*, 18−23.
64. Betz, S. F. (1993) *Protein Sci. 2*, 1551−1558.
65. Flory, P. J. (1956) *J. Am. Chem. Soc. 78*, 5222−5235.
66. Pace, C. N., Grimsley, G. R., Thomson, J. A., and Barnett, B. J. (1988) *J. Biol. Chem. 263*, 11820−11825.
67. Srinivasan, N., Sowdhamini, R., Ramahrishnan, C., and Balaram, P. (1990) *Int. J. Peptide Protein Res. 36*, 147−155.
68. Thornton, J. M. (1981) *J. Mol. Biol. 151*, 261−287.
69. Doig, A. J., and Williams, D. H. (1991) *J. Mol. Biol. 217*, 389−398.
70. Kuroki, R., Inaka, K., Taniyama, Y., Kidokoro, S., Matsushima, M., Kikuchi, M., and Yutani, K. (1992) *Biochemistry 31*, 8323−8328.
71. Schwarz, H., Hinz, H. J., Mehlich, A., Tscheche, H., and Wenzel, H. R. (1987) *Biochemistry 26*, 3544−3551.
72. Dill, K. A., and Shortle, D. (1991) *Annu. Rev. Biochem. 60*, 795−825.
73. Farrow, N. A., Zhang, O., Forman-Kay, J. D., and Kay L. E. (1995) *Biochemistry 34*, 868−878.
74. Cooper, A., Eyles, S. J., Redford, S. E., and Dobson, C. M. (1992) *J. Mol. Biol. 225*, 939−943.
75. Adby, P. R., and Dempster, M. A. H. (1974) *Introduction to Optimization Methods*, Wiley and Sons: New York.

BI971983O